NUCLEAR SCIENCE AND TECHNIQUES **26**, 030501 (2015)

Angle-resolved photoemission spectroscopy in Hubbard model based on cluster perturbation*

XUE Bing (薛冰),[1,2] REN Cui-Lan (任翠兰),[1] ZHANG Wei (张伟),[1] and ZHU Zhi-Yuan (朱志远)[1,†]

[1]*Shanghai Institute of Applied Physics, Chinese Academy of Sciences, Shanghai 201800, China*
[2]*Graduate University of Chinese Academy of Sciences, Beijing 100049, China*

(Received January 30, 2015; accepted in revised form April 15, 2015; published online June 20, 2015)

Angle-resolved photoemission spectra (ARPES) are calculated in the Hubbard model by using cluster perturbation method. It is found that in a cluster of 12 sites, the local density of states displays the phase transition from normal conductor to Mott insulator with the increase of the electron-electron coupling. We show that a pseudogap develops from the metallic phase to the insulating phase. Evidence of spin-charge separation is also verified in the calculated single particle spectral functions.

Keywords: Angle-resolved photoemission spectra, Cluster perturbation theory, Exact diagonalization

DOI: 10.13538/j.1001-8042/nst.26.030501

I. INTRODUCTION

As an important issue in condensed matter physics, strong correlations originating from electron-electron interactions are related to interesting phenomena of high temperature superconductivity, colossal magnetic resistance [1–3], and the metal-insulator transition known as Mott transition, to which extensive research efforts, theoretical [4, 5] and experimental [6–8], have been made. The studies on Mott transition are of great help in understanding some fundamental physical phenomena, such as high temperature superconducting.

Angle-resolved photoemission spectroscopy (ARPES) is a powerful tool to study the electronic structures in solids, even solids of strong electron-electron interactions [9–11]. Being of high energy and momentum resolution it enables bulk sensitive observation [12] and provides reliable information about electron structures of solids. It has been used to investigate many kinds of materials including the Mott insulators.

However, sometime theoretical calculations fail to give reasonable interpretations for ARPES experiments due to the strongly correlated electrons, where the usual approximations of many-body quantum mechanics become invalid for such systems. Among them, to describe properties of the low-dimensional strongly correlated cuperate material for ARPES experiments, the Hubbard model with nearest-neighbour hopping and on-site Coloumb repulsion is often used [13, 14]. To solve lattice models with local interaction, the cluster perturbation theory (CPT) is mostly used, especially for Hubbard model of half-filling or non-half-filling [15–18]. Such a method can be viewed as a cluster extension of strong-coupling perturbation theory. With the CPT method, we can deal with a lattice model of many more sites. We can calculate the Green's function with a given wave vector and obtain a large number of poles of the Green's function, hence a high spectrum resolution. In this paper, we studied the single particle spectral function of the low-dimensional Hubbard model with CPT method. The model and CPT approach, and the numerical results and discussion, are presented.

II. MODEL AND METHOD

A. Hubbard model

The Hubbard model is the basic model to describe systems of correlated electrons. It describes that electrons of spin σ can hop between sites on a lattice. Its Hamiltonian is given by

$$H = -t \sum_{\langle i,j\rangle;\sigma} (c^{\dagger}_{i\sigma} c_{j\sigma} + c^{\dagger}_{j\sigma} c_{i\sigma}) + U \sum_{i} n_{i\uparrow} n_{i\downarrow}, \quad (1)$$

where, $\langle i,j\rangle$ denotes the nearest-neighbor sites; t is the hopping energy; U is the on-site Coulomb repulsion; $c^{\dagger}_{i\sigma}$ and $c_{i\sigma}$ are creation and annihilation operators, respectively, for electrons of spin σ on site i; and $n_{i\sigma} = c^{\dagger}_{i\sigma} c_{i\sigma}$ is the electron number operator on site i. The average density of electron per site is $n = N_e/N$, where N is the number of sites, N_e is the number of electrons, and $n/2$ is the band filling. If $U = 0$, this model reduces to the tight-binding model; while if $U \geq t$, the strong repulsion suppresses states with more than one electron per site.

B. Cluster perturbation theory

The CPT theory is an approximation scheme applied to lattice models with local interactions. The basic idea is to divide the infinite lattice into identical disconnected clusters, with each cluster containing N lattice sites. The clusters can be solved exactly and the inter-cluster hopping terms are treated at the first order in strong-coupling perturbation theory. We use CPT to calculate one-particle properties of the Hubbard model. Exact diagonalization is applied to the unit cluster to calculate the Green's function and then extended to the full infinite lattice. The complete Hamiltonian of the system can

* Supported by the National Natural Science Foundation of China (No. 11075196)
† Corresponding author, zhuzhiyuan@sinap.ac.cn

be written as the sum of the one-body part H_0 and the interaction part V

$$H = H_0 + V, \tag{2}$$

$$H_0 = \sum_{\boldsymbol{R}} H_0^{\boldsymbol{R}}, \quad V = \sum_{\boldsymbol{R},\boldsymbol{R}',i,j} V_{ij}^{\boldsymbol{R}\boldsymbol{R}'} c_{\boldsymbol{R}i}^{\dagger} c_{\boldsymbol{R}'j}, \tag{3}$$

where $H_0^{\boldsymbol{R}}$ is the Hubbard Hamiltonian of the cluster corresponding to R which is the vector of the cluster superlattice and V is the nearest-neighbor hopping between adjacent clusters.

The quantity we are interested in is the one-particle Green's function, which is defined as

$$G(k,z) = G_{\mathrm{e}}(k,z) + G_{\mathrm{h}}(k,z), \tag{4}$$

$$G_{\mathrm{e}}(k,z) = \langle\Omega|c(k)\frac{1}{z-H+E_0}c^{\dagger}(k)|\Omega\rangle, \tag{5}$$

$$G_h(k,z) = \langle\Omega|c^{\dagger}(k)\frac{1}{z+H-E_0}c(k)|\Omega\rangle, \tag{6}$$

where, $z=\omega+i\eta$, $c^{\dagger}(k)$ and $c(k)$ are the creation and annihilation operators, respectively, on wave vector k; E_0 is the ground energy; and $|\Omega\rangle$ is the ground state. From Eqs. (4)–(6), one obtains the single-particle spectral function

$$A(k,\omega) = -2\lim_{\eta\to 0^+}\mathrm{Im}G(k,\omega+i\eta), \tag{7}$$

where $A(k,\omega)$ is the probability for an electron of momentum $\hbar k$ to have an energy $\hbar\omega$. The negative-frequency part of the function comes from G_h, which can be accessed by ARPES in experiments.

The lowest-order approximation of the full single-particle Green's function can be written as

$$G_{ij}(Q,z) = \left(\frac{G(z)}{1-V(Q)G(z)}\right)_{ij}, \tag{8}$$

where Q is the cluster superlattice wave vector, and $V(Q)$ is the Fourier transformation of the $N\times N$ hopping matrix. Finally the Green's function $G_{ij}(Q,z)$ can be transformed from the mixed representation to the real space within a cluster and reciprocal space between clusters. The lowest-order CPT approximation to the Green's function is

$$G(k,z) = \frac{1}{N}\sum_{i,j}\mathrm{e}^{-ik(i-j)}G_{ij}(Nk,z). \tag{9}$$

C. Basis states construction

For a lattice of N sites with $N_\uparrow$ spin up electrons and $N_\downarrow$ spin down electrons, the basis states are constructed as the creation operators acting on the vacuum state with a certain order. For the Hubbard model we sort the electrons first by the spin index and then by the site index. Here the spin up operators are set left to the spin down operators, and the site indices of the operators are chosen to increase from left to right

$$c_{1\uparrow}^{\dagger}c_{2\uparrow}^{\dagger}\cdots c_{i\uparrow}^{\dagger}\cdots c_{k-1\uparrow}^{\dagger}c_{k\uparrow}^{\dagger}c_{1\downarrow}^{\dagger}c_{2\downarrow}^{\dagger}\cdots c_{i\downarrow}^{\dagger}\cdots c_{k-1\downarrow}^{\dagger}c_{k\downarrow}^{\dagger}|\rangle = |N_{k\uparrow},N_{k-1\uparrow}\cdots N_{i\uparrow}\cdots N_{2\uparrow},N_{1\uparrow};N_{k\downarrow},N_{k-1\downarrow}\cdots N_i\cdots N_{2\downarrow},N_{1\downarrow}\rangle. \tag{10}$$

A site occupied by one electron is coded as 1, and otherwise as 0. Then the basis $|N_k,N_{k-1}\cdots N_i\cdots N_2,N_1\rangle$ can be coded each other with a binary number of $(N_kN_{k-1}\cdots N_i\cdots N_2N_1)$. Once we find all the basis states, we can apply the Hamiltonian to them to obtain the matrix elements.

D. Exact diagonalization

With the matrix representation of basis states and Hamiltonian H, we can obtain the ground state by the Lanczos algorithm, with only a few extreme eigenvalues of a sparse matrix when it is too large to be fully diagonalized.

The basic implementation of the Lanczos algorithm is to build a projection of the full Hamiltonian matrix H onto a Krylov subspace. Starting from a random initial normalized state $|\psi_0\rangle$, we construct the Krylov subspace by iteratively applying the matrix H

$$K = \mathrm{span}\{|\psi_0\rangle, H|\psi_0\rangle, H^2|\psi_0\rangle,\ldots,H^n|\psi_0\rangle\}. \tag{11}$$

Then we orthogonalize these states against each other to obtain a basis of the Krylov space from the following recursion relation

$$|\psi_{n+1}\rangle = H|\psi_n\rangle - a_n|\psi_n\rangle - b_n^2|\psi_{n-1}\rangle, \tag{12}$$

where $a_n = \frac{\langle\psi_n|H|\psi_n\rangle}{\langle\psi_n|\psi_n\rangle}$, $b_n^2 = \frac{\langle\psi_n|\psi_n\rangle}{\langle\psi_{n-1}|\psi_{n-1}\rangle}$, $b_0=0$ and $|\psi_{-1}\rangle=0$. At any given step, only three state vectors of $|\psi_{n+1}\rangle$, $|\psi_n\rangle$ and $|\psi_{n-1}\rangle$ are kept in memory.

The projected Hamiltonian matrix is tridiagonal and is formed by the coefficients a_n and b_n

$$T = \begin{bmatrix} a_0 & b_1 & 0 & 0 & \ldots & 0 \\ b_1 & a_1 & b_2 & 0 & \ldots & 0 \\ 0 & b_2 & a_2 & b_3 & \ldots & 0 \\ \vdots & \vdots & \vdots & \vdots & \ddots & \vdots \\ 0 & 0 & 0 & 0 & \ldots & a_{n-1} \end{bmatrix}. \tag{13}$$

The tridiagonal matrix can be diagonalized by standard routines designed to solve tridiagonal matrices. The iterations

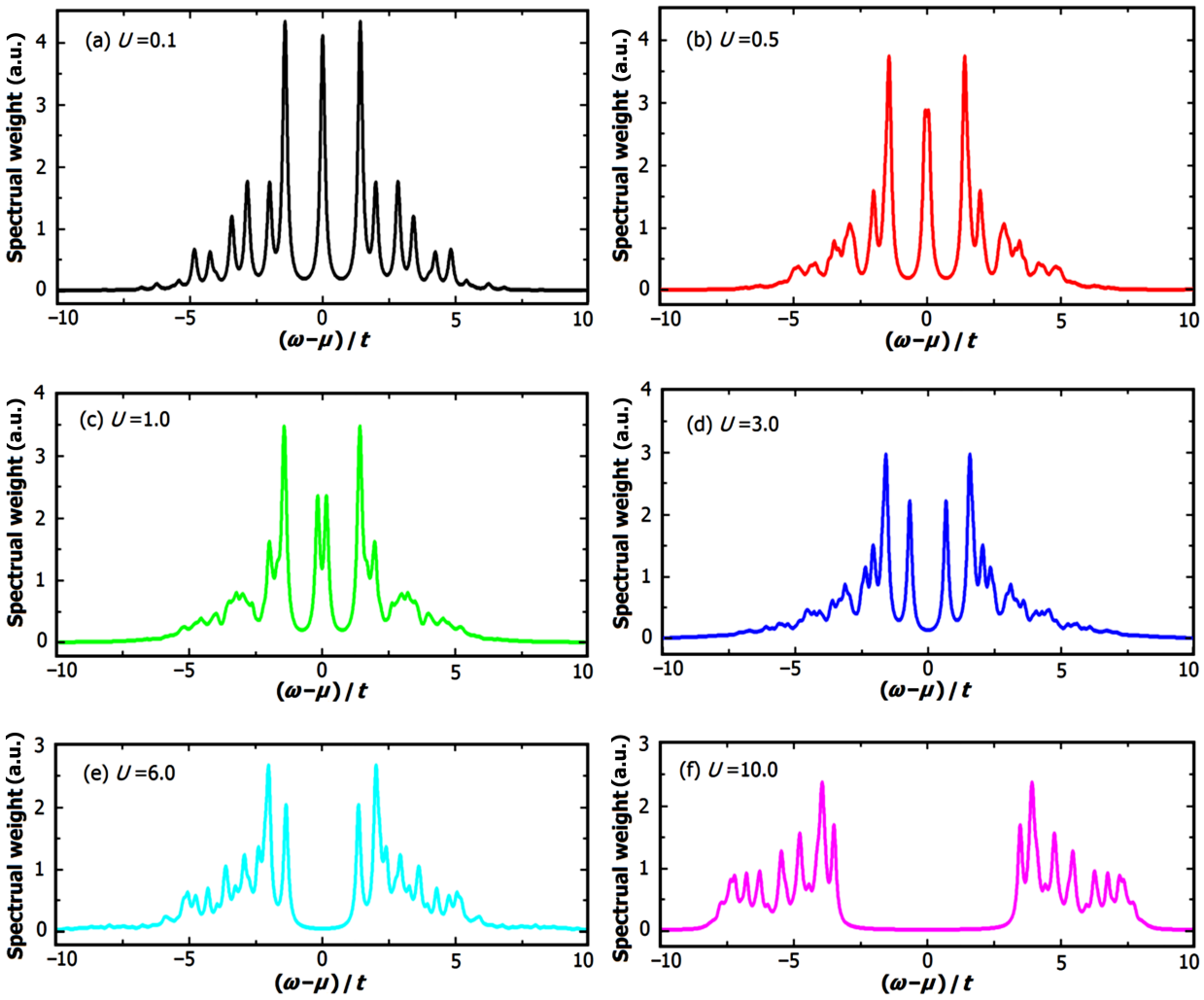

Fig. 1. (Color online) The density of state at different U values and half filling.

can be stopped when the residual $\|E_0|\Omega\rangle - H|\Omega\rangle\|$ is smaller than a preset tolerance.

The number of low lying eigenvalues that can converge is determined by the number of dimensions of the Krylov space. As the recursion order increases, the lowest eigenvalue and the corresponding eigenvector of the tridiagonal matrix T converges to the ground energy E_0 and ground state $|\Omega\rangle$ of the original Hamiltonian H. For the ground state $|\Omega\rangle$ is provided in the reduced basis $\{|\psi_n|\rangle\}$ and $\{|\psi_n|\rangle\}$ are not stored, we need to repeat the Lanczos recursion with the same initial vector $|\psi_0\rangle$ and construct the ground state progressively at each iteration from the coefficients $\langle\Omega|\psi_n\rangle$.

Convergence of the Lanczos algorithm is fast at the spectrum edge where the extreme eigenvalues are separated from each other, but worsen in the spectrum rapidly. So the Lanczos algorithm is only suitable to obtain the ground state and a few low lying excited states. A small number of iterations, varying from a few tens to 200, is sufficient in most cases.

III. RESULTS AND DISCUSSION

In this section, we apply the cluster perturbation method to investigate the spectral properties of one-dimensional half-filled Hubbard model of 12 sites, which is the largest size that we can perform a systematic study. As will be seen below, the essential feature of strongly coupled electronic systems can be well captured in our calculation. In the numerical work, we make electron hopping energy t as the unit of energy. The band width of our system is $4t$. In real solids the band width is a few eV. So the hopping energy t is estimated to 1 eV or so. In our calculation, we assume that the parameter η is 0.1 and the δ peak is of a finite width.

Figure 1 shows the local density of states $N(\omega)$ at different U values. Here, $N(\omega)$ is obtained by a summation over the electron spectral function $A(k,\omega)$ of different momenta. From Fig. 1, three stages of evolution are observed with increasing U. Figures 1(a) and 1(b) correspond to a gapless phase, where the electronic states are characterized by a continuum around the Fermi energy ($\omega = 0$) in the spectra. Fig-

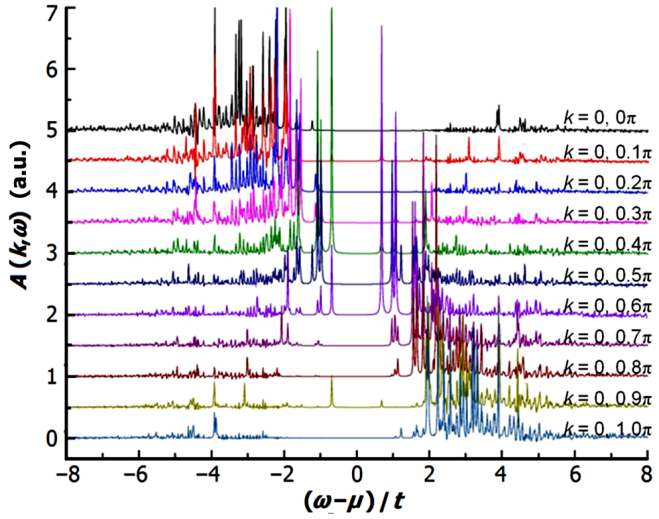

Fig. 2. (Color online) Single particle spectral function with different wave vectors from $k = (0, 0)$ to $k = (0, \pi)$ at $U = 3$ and half-filling.

ures 1(c) and 1(d) correspond to a pseudogap phase, where $N(\omega)$ shows a small dip at the Fermi energy, indicating the existence of a pseudogap structure. If we further increase U, the depth and width of the pseudogap continue growing and finally a well-defined Mott insulating gap appears, which corresponds to a gapped phase as seen in Figs. 1(e) and 1(f). This fully gapped state shows up when U is larger than $3t$. At the same time, the position of the inner and Hubbard bands almost remain unchanged. We can see that the results of $N(\omega)$ in Fig. 1 describe a clear metal-insulator transition from a normal metallic state at weak coupling to a Mott-Hubbard insulator at strong coupling.

Figure 2 presents the single-particle spectral functions at different values of wave vector k and $U = 3$. These momentum-dependent spectra provide extensive overview on the electronic band dispersion and band structures. Since the U is large, a Mott gap is almost developed at the Fermi energy. All the spectra are separated into two parts on the positive and negative energy sides. The distance between the upper and lower parts changes with k and reaches a minimum at $k = \pi/2$.

As mentioned in Section I, the spectral function has a direct correspondence with experimental photoemission and inverse photoemission spectra. The former detects the occupied states in electronic bands, and can be compared with the lower part in the calculated spectra below Fermi energy. Likewise, the latter offers an insight into the unoccupied electronic states above Fermi energy. Therefore, our theoretical results of pseudogap state and gap opening phenomenon in strongly correlated electronic systems can, in principle, be checked by experiments [19]. As shown in Fig. 2 of Ref. [19], a sharp dip of spectral density of state is observed at 30 K, and it increases at 15 K. The dip at Fermi energy indicates the pseudogap at low temperature. In Fig. 1 this pseudogap can be found when U is comparable to t.

In addition to the Mott gap, another interesting property shown in the spectra is the spin-charge separation. The interacting 1D electronic system is known as a Luttinger liquid, in which the elementary excitations are the independent waves of spins and charges, with its energy quanta being spinon and holon. They travel through the media at different speeds and possess distinct dispersion relations. These behaviors are also observable in the single-particle spectral function, which describes the excited states of Luttinger liquid on adding or removing an electron. In Fig. 2, the upper and lower parts of the spectrum are composed of two sub-structures with different energy dispersions, being consistent with the Luttinger liquid theory on spin-charge separation. These behaviors can be observed in experiments [20]. The high energy edge of spectral function is related to the spin excitation, and the low energy edge is related to the charge excitation.

IV. SUMMARY

In this work, we use the cluster perturbation theory to calculate the Green's function and single particle spectral function of strongly correlated electronic systems. By applying this theory, we study the spectral properties of Hubbard model at half-filling. The calculated local density of states displays a smooth evolution related to a phase transition from normal conductor to Mott insulator. Meanwhile, spin-charge separation is evidently verified in our calculations. These presented results are expected to be helpful for understanding experimental ARPES.

ACKNOWLEDGEMENTS

We thank Prof. HUAI Ping for his helpful discussion from beginning of this work. We also acknowledge the Shanghai Supercomputer Center for providing computing resources.

[1] Lanzara A, Bogdanov P V, Zhou X J, *et al*. Evidence for ubiquitous strong electron-phonon coupling in high-temperature superconductors. Nature, 2001, **412**: 510–514. DOI: 10.1038/35087518

[2] Yokoya T, Kiss T, Chainani A, *et al*. Fermi surface sheet-dependent superconductivity in 2H-$NbSe_2$. Science, 2001, **294**, 2518–2520. DOI: 10.1126/science.1065068

[3] Zhou X J, Yoshida T, Lanzara A, *et al*. High-temperature superconductors: Universal nodal Fermi velocity. Nature, 2003, **423**: 398. DOI: 10.1038/423398a

[4] Georges A, Kotliar G, Krauth W, *et al*. Dynamical mean-field theory of strongly correlated fermion systems and the limit of infinite dimensions. Rev Mod Phys, 1996, **68**: 13–125. DOI: 10.1103/RevModPhys.68.13

[5] Jarrell M. Hubbard-model in infinite dimensions: A quantum Monte-Carlo study. Phys Rev Lett, 1992, **69**: 168–171. DOI: 10.1103/PhysRevLett.69.168

[6] Makino H, Inoue I H, Rozenberg M J, *et al*. Bandwidth control in a perovskite-type $3d^1$-correlated metal $Ca_{1-x}Sr_xVO_3$. II. Optical spectroscopy. Phys Rev B, 1998, **58**: 4384–4393. DOI: 10.1103/PhysRevB.58.4384

[7] Perfetti L, Georges A, Florens S, *et al*. Spectroscopic signatures of a bandwidth-controlled Mott transition at the surface of $1T$-$TaSe_2$. Phys Rev Lett, 2003, **90**: 166401. DOI: 10.1103/Physrevlett.90.166401

[8] Sekiyama A, Fujiwara H, Imada S, *et al*. Mutual experimental and theoretical validation of bulk photoemission spectra of $Sr_{1-x}Ca_xVO_3$. Phys Rev Lett, 2004, **93**: 156402. DOI: 10.1103/Physrevlett.93.156402

[9] Gweon G H, Sasagawa T, Zhou S Y, *et al*. An unusual isotope effect in a high-transition-temperature superconductor. Nature, 2004, **430**: 187–190. DOI: 10.1038/Nature02731

[10] Eguchi R, Kiss T, Tsuda S, *et al*. Bulk and surface sensitive high-resolution photoemission study of Mott-Hubbard systems $SrVO_3$ and $CaVO_3$. Physica B, 2006, **378–380**: 330–331. DOI: 10.1016/j.physb.2006.01.120

[11] Damascelli A, Hussain Z and Shen Z X. Angle-resolved photoemission studies of the cuprate superconductors. Rev Mod Phys, 2003, **75**: 473–541. DOI: 10.1103/RevModPhys.75.473

[12] Shen Z X, Spicer W E, King D M, *et al*. Photoemission-studies of high-T_C superconductors: the superconducting gap. Science, 1995, **267**: 343–350. DOI: 10.1126/science.267.5196.343

[13] Li Q M, Callaway J and Tan L. Spectral function in the two-dimensional Hubbard model. Phys Rev B, 1991, **44**: 10256. DOI: 10.1103/PhysRevB.44.10256

[14] Dagotto E. Correlated electrons in high-temperature superconductors. Rev Mod Phys, 1994, **66**: 763–840. DOI: 10.1103/RevModPhys.66.763

[15] Pairault S, Sénéchal D and Tremblay A M S. Strong-coupling expansion for the Hubbard model. Phys Rev Lett, 1998, **80**: 5389–5392. DOI: 10.1103/PhysRevLett.80.5389

[16] Sénéchal D, Perez D and Pioro-Ladrière M. Spectral weight of the Hubbard model through cluster perturbation theory. Phys Rev Lett, 2000, **84**: 522. DOI: 10.1103/PhysRevLett.84.522

[17] Sénéchal D, Perez D and Plouffe D. Cluster perturbation theory for Hubbard models. Phys Rev B, 2002, **66**: 075129. DOI: 10.1103/Physrevb.66.075129

[18] Sénéchal D and Tremblay A M S. Hot spots and pseudogaps for hole- and electron-doped high-temperature superconductors. Phys Rev Lett, 2004, **92**: 126401. DOI: 10.1103/Physrevlett.92.126401

[19] Medicherla V R R, Patil S, Singh R S, *et al*. Origin of ground state anomaly in LaB_6 at low temperatures. Appl Phys Lett, 2007, **90**: 062507. DOI: 10.1063/1.2459779

[20] Kim C, Matsuura A Y, Shen Z X, *et al*. Observation of spin-charge separation in one-dimensional $SrCuO_2$. Phys Rev Lett, 1996, **77**: 4054–4057. DOI: 10.1103/PhysRevLett.77.4054